

## Arsenic adsorption by polyvinyl pyrrolidone K25 coated cassava peel carbon from aqueous solution

R. Selvakumar<sup>a,\*</sup>, S. Kavitha<sup>a</sup>, M. Sathishkumar<sup>b</sup>, K. Swaminathan<sup>a</sup>

<sup>a</sup> Microbial Biotechnology Division, Department of Biotechnology, Bharathiar University, Coimbatore 641046, Tamil Nadu, India

<sup>b</sup> Department of Food Science and Technology, College of Agriculture, Chonbuk National University, Chonju 561-756, South Korea

Received 8 November 2006; received in revised form 8 August 2007; accepted 9 August 2007

Available online 12 August 2007

### Abstract

Sorption of arsenic from aqueous solution was carried out using polyvinyl pyrrolidone K25 coated cassava peel carbon (PVPCC). Batch experiments were conducted to determine the effect of contact time, initial concentration, pH and desorption. Batch sorption data's were fitted to Lagergren kinetic studies. Column studies were also conducted using PVPCC as adsorbent. The optimized flow rate of 2.5 mL min<sup>-1</sup> and bed height 10 cm were used to determine the effect of metal ion concentration on removal of As(V). BDST model was applied to calculate the adsorption capacity ( $N_0$ ) of column. The  $N_0$  value of  $2.59 \times 10^{-5}$ ,  $4.21 \times 10^{-5}$ ,  $4.05 \times 10^{-5}$ ,  $4.26 \times 10^{-5}$  and  $3.2 \times 10^{-5}$  mg g<sup>-1</sup> were obtained for 0.5, 1.0, 1.5, 2.0 and 2.5 mg L<sup>-1</sup> of As(V), respectively. The batch sorption proved to be more efficient than the column sorption. The sorption of As(V) and the nature of the adsorbent was examined by Fourier transmission infrared spectroscopy (FTIR) and X-ray diffraction (XRD) studies, respectively. © 2007 Elsevier B.V. All rights reserved.

**Keywords:** PVP K25; As(V); Cassava carbon; XRD; FTIR studies

### 1. Introduction

Ground water contamination by arsenic has been a major problem in the northeastern parts of India like West Bengal, Assam and in few pockets of Orissa where continuous consumption of arsenic contaminated water has lead to hyperkeratosis, skin cancers and pigmentation of palm. Due to these clinical manifestations caused by the arsenic contaminated drinking water World Health Organization (WHO) has recommended 0.01 mg L<sup>-1</sup> as maximum contaminant level (MCL) in drinking water [1].

Considering its clinical significance, extensive studies have been carried out for As(III) and As(V) removal using various methods like precipitation [2], ion exchange [3] and adsorption [4]. Scientific evidences suggested that adsorption is an efficient method to control the mobility and bioavailability of arsenic when compared to other methods. Adsorption of arsenic has been tried with various adsorbents like activated carbon [4], calcium chloride (CaCl<sub>2</sub>) impregnated rice husk carbon [5],

FeSO<sub>4</sub> and CuSO<sub>4</sub> doped coir pith carbon [6], natural laterite [7], nanoscale zerovalent iron [8], sulphate modified iron oxide coated sand [9], orange juice residues [10], iron oxide loaded alginate beads [1], mixed rare earth oxides [11], activated neutralized red mud [12], modified mycelial pellets of *Aspergillus fumigatus* [13], pretreated tea fungal biomass [14], fresh and immobilized plant biomass [15] and iron containing mesoporous carbon [16].

Polymer composites play important role in today's adsorption technology. Arsenic removal has been tried with metal loaded polymers, strong cation exchange resins, macro porous polymers, chelating resins or biopolymer gels [17]. Lenoble et al. [18] have reported that MnO<sub>2</sub> loaded polystyrene resins were effective in oxidizing As(III) to As(V) and observed increased removal. DeMarco et al. [19] developed a hybrid polymeric/inorganic sorbent made of Purolite C-145 resin that was compatible with fixed bed column process with excellent mechanical strength and attrition resistant properties. ArsenX<sup>np</sup>, a hybrid sorbent consisting of nanoparticle of hydrous iron oxide distributed throughout a porous polymer bead was used for arsenic removal [20]. Zr(IV) EDTA complex was immobilized on chloromethylated polystyrene beads for removal of oxoanions of As(III), As(V) and Se(IV) compounds [21]. Deng and

\* Corresponding author. Tel.: +91 422 2424865.

E-mail address: [selvabiotech@gmail.com](mailto:selvabiotech@gmail.com) (R. Selvakumar).

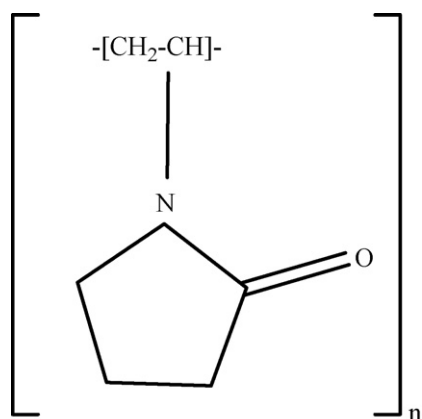


Fig. 1. Structure of PVP monomer.

Ting [22] grafted *Penicillium chrysogenum* with polyethylenimine for removal of As(III) and As(V) from water. A hybrid polymer/inorganic fibrous sorbent was developed to remove arsenic from drinking water [23]. Rivas et al. [24] developed a water soluble polymer conjugated ultra filtration membrane to remove arsenate ions.

Polyvinyl pyrrolidone (PVP) (Fig. 1), an organic polymer has been used as an intermediate sizing material to increase the adhesion property of carbon fiber to vinyl ester matrix. The inter-diffusion of PVP had been a key factor in improving the adhesion property of the carbon fiber [25]. PVP is currently used in the adsorption of different polyphenols from apple juices and the mechanism of adsorption mainly relies on carbonyl adsorption sites of PVP [26]. PVP is used in pharma industry for preparing blends of different drug especially in controlled drug release delivery systems [27]. Poly(4-vinyl pyridine) has been used as a coating agent on silica gel for chromium removal [28]. Similar reports are available for Uranyl sulphate recovery using poly(4-vinyl pyridine) cross linked silica gel [29].

In the present study, cassava peel, an agricultural waste from food processing industry has been used for the preparation of activated carbon for the removal of arsenic from aqueous solution. Adsorption of As(V) by PVP K25 coated cassava peel (PVPCC) carbon was investigated in batch and column studies. Early preliminary studies revealed that PVPCC was less efficient in As(III) removal when compared to As(V) (unpublished data). Further, experiments were carried out using As(V) only. Efficiency of PVPCC to adsorb arsenate from aqueous solution was studied by applying the experimental data to Lagergren kinetics. The interaction of arsenate with PVPCC surface and the morphological features of these adsorbents were analysed using FTIR and XRD studies, respectively.

## 2. Experimental

### 2.1. Materials and methods

Waste cassava peel was collected from sago industries and washed with generous amount of tap water to remove bound earthen materials and dried in sunlight. The cassava peel was sieved to 125–250  $\mu\text{m}$  size and filled in a steel container with

Table 1  
Properties of PVP K25

Properties	PVP K25
Intrinsic viscosity ( <i>K</i> -value)	20–30
pH of 5% solution	3–5
Nitrogen content	11.5–12.8%
Sulphated ash	0.1%
Heavy metals	0.001%
Molecular formula	(C <sub>6</sub> H <sub>9</sub> NO) <sub>n</sub>
Molecular weight	(111.15) <sub>n</sub>

a tight lid. The inner space was filled with sand, which was consolidated layer by layer to the brim of the container. The setup was subjected to carbonization at 700 °C for 1 h using muffle furnace under closed conditions. After carbonization, the activated carbon was taken out and sieved to a mesh size of 125–250  $\mu\text{m}$  again and used for adsorption studies. All the chemicals used in the study were of analytical reagent grade and procured from Merck, Himedia, SD Fine and Qualigens, Mumbai.

### 2.2. PVP coating and property analysis

PVP coating was carried out according to Manju et al. [30]. In brief, a known quantity of thermally activated cassava peel carbon was added to 0.1 M PVP K25 and agitated on a rotary shaker with a speed of 150 rpm for 48 h at room temperature. The properties of the PVP K25 used in the experiment are given in Table 1. The PVP K25 coated carbon was filtered and dried at 80 °C. Further, PVPCC was subjected to property analysis according to Selvakumari [31] and are tabulated (Table 2).

### 2.3. Spectrophotometric determination of As(V)

As(V) estimation was carried out according to Lenoble et al. [32]. In brief, a known quantity of ammonium molybdate was mixed with 9 M sulphuric acid making up to 100 mL and named as 'Reagent A'. Ten percent ascorbic acid was prepared daily before use. As(V) estimation was carried out using a known quantity of ascorbic acid solution and 2 mL reagent A and successively added to a 40 mL sample aliquot in a 50 mL volumetric flask. The volume was completed by deionised water. A blank was prepared according to the same procedure using the appropriate volume of deionised water. The minimum detection limit of As(V) determination by this method is 20  $\mu\text{g L}^{-1}$ . The anal-

Table 2  
Properties of PVP K25 coated cassava carbon

Properties	PVPCC
Conductivity ( $\mu\text{S cm}^{-1}$ )	0.230
Moisture (%)	19.99
Decolorizing power ( $\text{mg g}^{-1}$ )	3.0
Specific gravity ( $\text{W}_a \text{V}^{-1}$ )	1.28
Apparent density	0.251
Ion exchange ( $\text{Me g}^{-1}$ )	0.2
Surface area ( $\text{m}^2 \text{g}^{-1}$ )	296

ysis was carried out in 1 cm quartz cells with a Shimadzu 1601 UV–vis spectrophotometer.

#### 2.4. Batch mode studies

Batch mode studies were carried out by agitating 100 mg of adsorbent with 50 mL of As(V) solution of desired concentration and pH at 150 rpm in a rotary shaker at room temperature. Concentration of As(V) was estimated spectrophotometrically. The samples were withdrawn from the shaker at predetermined time intervals, supernatant solution was separated from the adsorbent by centrifugation at 15,000 rpm for 20 min and the remaining arsenate was analysed. Effect of pH was studied in the range of 2–11 by adjusting the pH of the solution using 0.1N HCl and NaOH solutions. The initial concentration of 2.0 mg L<sup>-1</sup> of arsenate solution and 100 mg 50 mL<sup>-1</sup> of adsorbent dose was used to examine the pH effect. Lagergren kinetics was employed to study the adsorption equilibrium.

#### 2.5. Column mode studies

The efficiency of PVPCC for As(V) adsorption in column mode was studied. 2.5 cm bed height of adsorbent was packed in a glass column (30 cm × 4.2 cm) and the 2.0 mg L<sup>-1</sup> As(V) solution was adjusted to a flow rate of 2.5, 5.0, 7.5 and 10 mL min<sup>-1</sup>. Fractions were collected at regular time intervals and analysed for As(V). The study was repeated with best flow rate and bed height with different As(V) concentration (0.5, 1.0, 1.5, 2.0 and 2.5 mg L<sup>-1</sup>) to determine the effect of concentration on As(V) removal. Data obtained were used to plot BDST curves and adsorption rate constant ( $N_0$ ) was calculated from the plot. Bed-depth-service-time model (BDST), proposed by Hutchins [33] is a simple method to correlate the service time,  $t$ , with process variables in fixed bed absorber.

$$C_0 t = \frac{N_0}{uH} - \left\{ \frac{1}{k_a x} \ln \left( \frac{C_0}{C_t - 1} \right) \right\} \quad (1)$$

where  $t$  is service time to breakthrough (min),  $N_0$  the adsorption capacity (mg L<sup>-1</sup>) of the adsorbent bed,  $C_0$  the influent concentration (mg L<sup>-1</sup>),  $u$  the linear flow rate (mg min<sup>-1</sup>),  $H$  the depth of the bed (cm),  $k_a$  the rate constant of adsorption (L<sup>-1</sup> min<sup>-1</sup> mg<sup>-1</sup>), and  $C_t$  is the effluent concentration at time  $t$  (mg L<sup>-1</sup>).

#### 2.6. Desorption studies

The adsorbent that was used for the adsorption of 2.0 mg L<sup>-1</sup> of As(V) was separated by centrifugation. The As(V) loaded adsorbent was filtered through Whatman No. 1 filter paper and washed gently to remove any unadsorbed arsenic. Several such samples were prepared and the spent adsorbent was mixed with 50 mL of distilled water at different pH values (2–11) adjusting the pH of the solution using 0.1N HCl and NaOH solutions and agitated at equilibrium time. The desorbed arsenic was estimated spectrophotometrically. The experiments were carried out in duplicate and mean values are taken for calculations.

#### 2.7. FTIR and XRD analysis

The FTIR analysis was carried out using with Shimadzu model FTIR-8201 PC. FTIR spectra were obtained at a scanning speed of 2 mm s<sup>-1</sup> at a resolution of 4 cm<sup>-1</sup>. The completely dried samples were treated with spectral grade KBr for pelletting. The morphological features of PVPCC and As(V) laden PVPCC were determined by X-ray diffraction analysis using Philips 6000 Diffractometer using filtered copper K $\alpha$  radiation. The prepared samples were analysed at drive axis of  $2\theta$  in the range of 10–80° in continuous mode. The scan speed was 5.0° min<sup>-1</sup>.

### 3. Results and discussion

#### 3.1. Effect of contact time and initial concentration on As(V) adsorption

PVPCC showed effective As(V) removal in aqueous solution. However, the initial adsorption studies revealed that the PVPCC was inefficient in removal of As(III) and need to be oxidized to As(V) before adsorption process. Further, the experiments were continued with As(V) solution only. At maximum As(V) concentration, PVPCC was efficient 2.53-folds the native one. The As(V) uptake was found to increase with increase in contact time and remained constant after equilibrium. The equilibrium time was found to be 45, 60, 105, 120 and 150 min for 0.5, 1.0, 1.5, 2.0 and 2.5 mg L<sup>-1</sup> of As(V) concentration, respectively. The percent removal at equilibrium decreased from 100 to 88.53% as the concentration increased from 0.5 to 2.5 mg L<sup>-1</sup> (Fig. 2). The initial rapid phase may be due to increased number of vacant sites available for adsorption at initial stages, as a result their exists increased concentration gradient between adsorbate in solution and adsorbate in adsorbent [34].

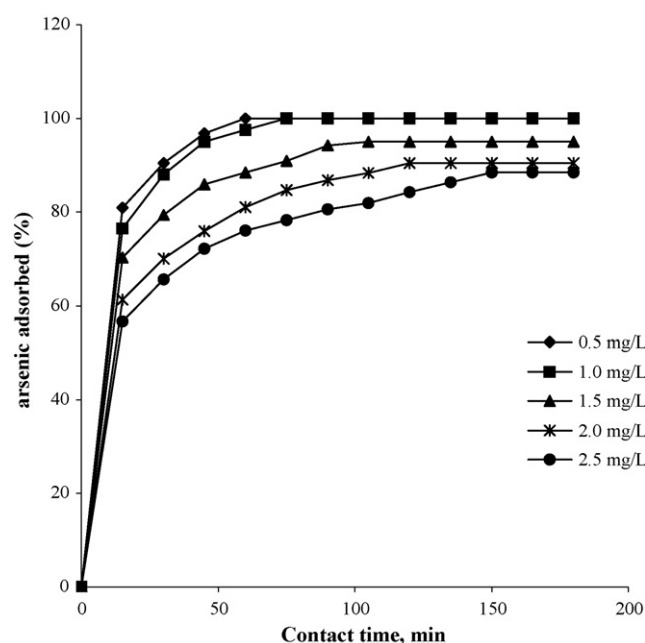


Fig. 2. Effect of agitation time and concentration of As(V) on removal.

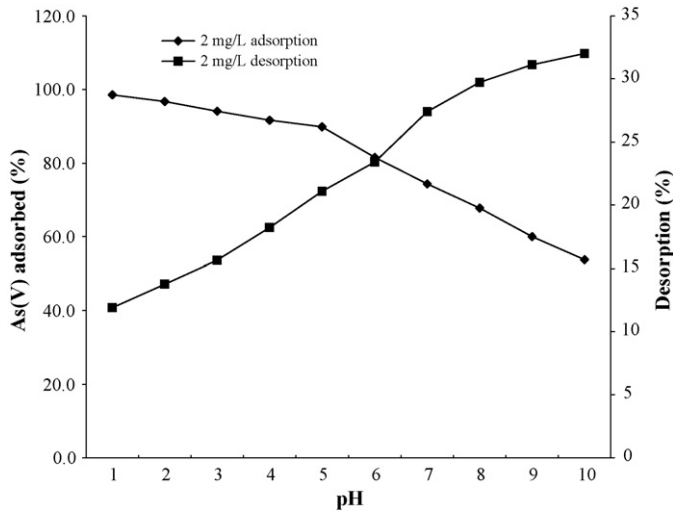


Fig. 3. Effect of pH on adsorption and desorption of As(V).

### 3.2. Effect of pH on As(V) adsorption

The extent of adsorption of ions is strongly influenced by the pH of the solution. The effect of pH on removal of As(V) is shown in Fig. 3. The percent removal was more than 90% in the pH range of 2–5 where after the percentage removal decreased. Higher adsorption at pH 2 could be related to the strong electrostatic attraction between positively charged surface sites for the predominant As(V) species  $\text{H}_2\text{AsO}_4^-$ , whereas a decrease of As(V) adsorption above pH 7 could be due to electrostatic repulsion between the negatively charged As(V) species,  $\text{HAsO}_4^{2-}$ , and the adsorbent surface [35]. Since the pH range where the monovalent arsenate is predominant as shown in Fig. 4 are almost identical to that where high removal of As(V) is achieved as shown in Fig. 3, it can be concluded that an effective removal of As(V) from aqueous solution can be accompanied by using PVPCC. Our result is in harmony with previous findings [10,11,12,22,23,36,37].

### 3.3. Adsorption kinetics

#### 3.3.1. Lagergren rate constant

The adsorption kinetics data of As(V) was analysed using the Lagergren first order rate equation. The rate constant of adsorp-

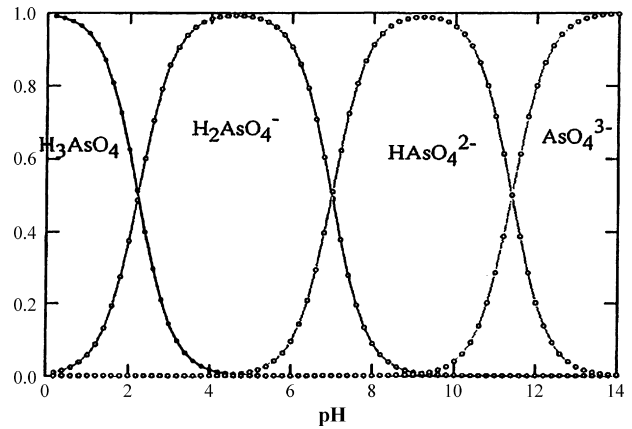


Fig. 4. Speciation diagram of As(V) as functions of pH [36].

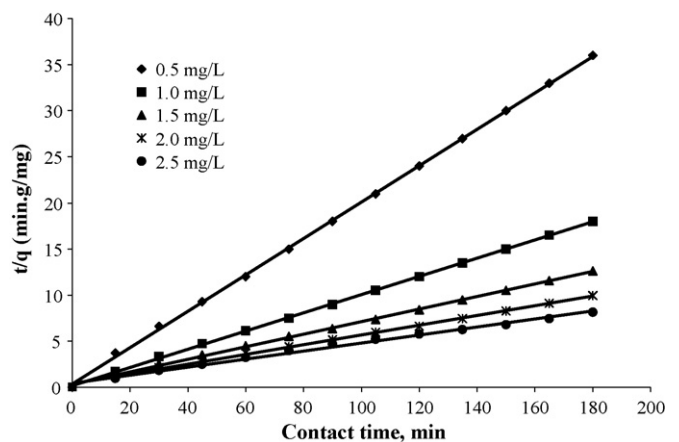


Fig. 5. Second order kinetic plot for the removal of As(V) at different concentrations (adsorbent dosage, 100 mg/50 mL; pH, 5.0; temperature, 30 °C).

tion is determined from the following first order rate expression [38].

$$\log(q_e - q) = \frac{\log q_e - k_{ad}}{2.303 \times t} \quad (2)$$

where  $q$  and  $q_e$  are amount of metal adsorbed ( $\text{mg g}^{-1}$ ) at time,  $t$  min and at equilibrium, respectively.  $k_{ad}$  is the rate constant for adsorption ( $\text{min}^{-1}$ ).

It was found that the calculated  $q_e$  do not agree with the experimental  $q_e$  values. This shows that the adsorption of As(V) does not follow pseudo first order kinetics. The second order

Table 3  
Lagergren kinetic parameters for the removal of As(V) by PVPCC

Initial As(V) concentration ( $\text{mg L}^{-1}$ )	$q_e$ (Exp.) ( $\text{mg g}^{-1}$ )	First order kinetic model			Second order kinetic model		
		$k_1$ ( $\text{L min}^{-1}$ )	$q_e$ (cal.) ( $\text{mg g}^{-1}$ )	$R^2$	$k_2$ ( $\text{g mg}^{-1} \text{min}^{-1}$ )	$q_e$ (cal.) ( $\text{mg g}^{-1}$ )	$R^2$
0.5	5.0	0.0596	2.50	0.9832	0.0138	5.06	0.9997
1.0	10.0	0.0368	2.47	0.9971	0.0018	10.12	0.9997
1.5	14.26	0.0405	8.31	0.9101	0.0014	14.66	0.999
2.0	18.10	0.0288	9.88	0.9943	0.0011	18.90	0.9977
2.5	22.13	0.0140	8.49	0.9648	0.0009	23.04	0.9926



kinetic model [39] can be represented as

$$\frac{t}{q} = \frac{1}{k_2 q_e} + \frac{t}{q_e} \quad (3)$$

where  $k_2$  is the equilibrium rate constant of pseudo second order adsorption ( $\text{g mg}^{-1} \text{min}^{-1}$ ). Values of  $k_2$  and  $q_e$  were calculated from the plot of  $t/q$  vs.  $t$  (Fig. 5). The calculated  $q_e$  values agrees with experimental  $q_e$  values and also, the correlation coefficient for the second order kinetic plot at all the studies concentration were above 0.99 (Table 3). These results show that the adsorption system studied belongs to the second order kinetic model. A similar phenomenon has been observed in the adsorption of As(V) and As(III) onto PEI modified *P. chrysogenum* [22], methylene blue by coir pith carbon [34], Cr(VI) onto sawdust [40] and congo red onto coir pith carbon [41].

### 3.4. Column studies

#### 3.4.1. Effect of flow rate and bed volume on As(V) adsorption

Increasing the flow rate decreased the removal of As(V) and after a certain period removal was nil. The removal was ceased at 390 min for flow rate  $2.5 \text{ mL min}^{-1}$ ; 150 min for flow rate  $5.0 \text{ mL min}^{-1}$ ; 90 min for flow rate  $7.5 \text{ mL min}^{-1}$  and 60 min for flow rate  $10.0 \text{ mL min}^{-1}$ . Initially at 15 min 100, 86.4, 63.2 and 48.6% of As(V) was removed with the flow rate of 2.5 mL to  $10.0 \text{ mL min}^{-1}$ , respectively but the removal decreased with increase in time (Fig. 6). The increase in flow rate decreases the contact time between the adsorbate and adsorbent, but increases the volume contacting the adsorbent. When the available adsorption sites all have been used, metal removal process terminates. The rate of adsorption decreases as time was increased. Our results are in correlation with previous findings [42,43].

The effect of bed volume on As(V) adsorption was studied with  $2 \text{ mg L}^{-1}$  of As(V) concentration at a flow rate of  $2.5 \text{ mL min}^{-1}$  and increasing bed volume of 34.82, 69.24, 103.86 and  $138.86 \text{ cm}^3$ . The As(V) removal was found to increase from 71.21, 100, 100 and 100% for increasing bed volume of 34.82, 69.24, 103.86 and  $138.86 \text{ cm}^3$ , respectively. The removal was ceased at an effluent volume of 600, 1050, 1162.5

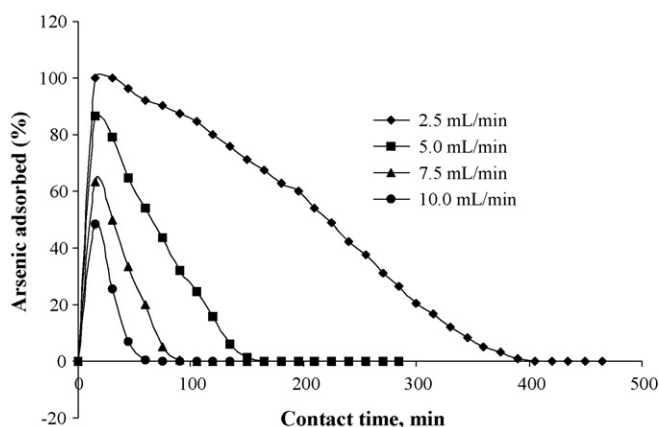


Fig. 6. Effect of flow rate on As(V) removal by PVPCC.

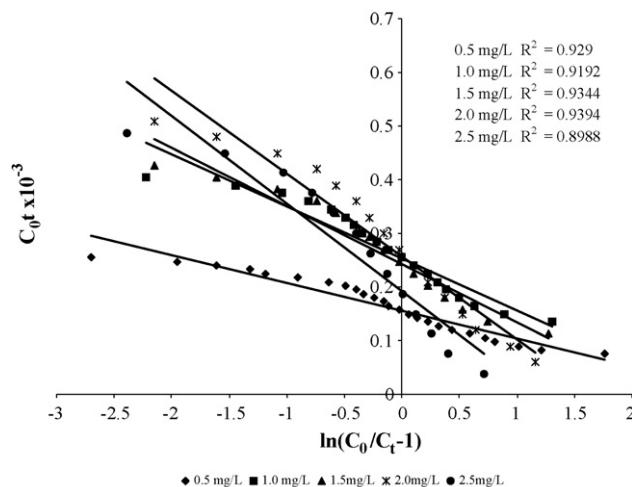


Fig. 7. BDST plots for As(V) removal by PVPCC.

and  $1387.5 \text{ mL}$  for 34.82, 69.24, 103.86 and  $138.86 \text{ cm}^3$  bed volume, respectively, beyond which no adsorption took place. The results shows that the number of available sites for As(V) adsorption increased with increase in bed volume owing to the increased amount of effluent volume with higher percent removal. The percent removal decreased as the contact time was increased depicting the phenomenon of site saturation. The empty bed contact time (EBCT) was considered as the time that the water needs to fill the empty column and was calculated according to the following equation [1].

The EBCT for As(V) adsorption was found to be 13.93, 6.96, 4.64 and 3.48 min for a flow rate of 2.5, 5.0, 7.5 and  $10.0 \text{ mL min}^{-1}$ , respectively with a constant bed volume of  $34.82 \text{ cm}^3$ . When the bed volume was increased from 34.82 to  $138.86 \text{ cm}^3$  keeping the flow rate ( $2.5 \text{ mL min}^{-1}$ ) as constant, the EBCT increased. The EBCT was observed to be 13.93, 27.69, 41.54 and 55.54 min with increasing bed volume of 34.82, 69.24, 103.86 and  $138.86 \text{ cm}^3$ , respectively. At optimum flow rate of  $2.5 \text{ mL min}^{-1}$  and bed volume of  $138.86 \text{ cm}^3$ , the EBCT was 55.54 min and the As(V) removal in empty bed was found to be below the detection limit.

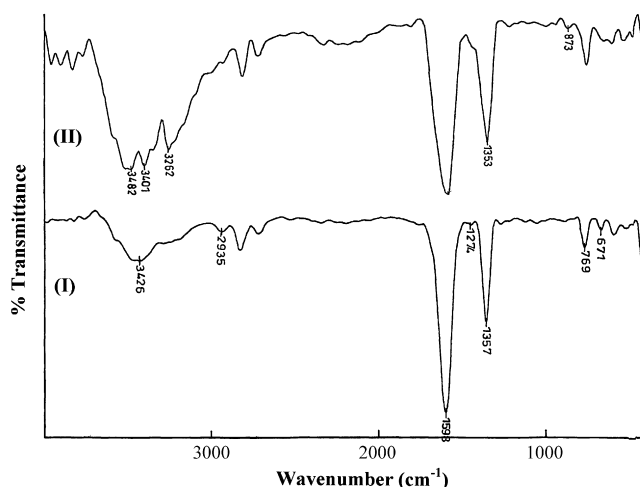


Fig. 8. FTIR spectra of carbon: (I) FTIR spectra of PVPCC; (II) FTIR spectra of As(V) laden PVPCC.

Table 4  
Comparison of FTIR spectra of As(V) laden PVPCC with earlier adsorbents in literature

Adsorbent	FTIR peaks ( $\text{cm}^{-1}$ )	Species	Description	References
Amorphous aluminium oxide	862	As(V)	As–O stretch	[46]
Amorphous ferric oxide	824	As(V)	As–OH stretch	[46]
Akaganeite type nanocrystal	850	As(V)	–	[47]
Goethite	834	As(V)	As–OH stretch	[48]
Hydrous iron oxides	878	As(V)	–	[49]
PVPCC	873.596	As(V)	As–O stretch	Present study

### 3.4.2. BDST plot

Fig. 7 shows a linear plot, suggesting the fixed bed volume of As(V) obeys the BDST model. Adsorption rate constant  $K_a$  and  $N_0$  were calculated from the slope and intercept of BDST plot.  $N_0$  value for As(V) adsorption by PVPCC was  $2.59 \times 10^{-5}$ ,  $4.21 \times 10^{-5}$ ,  $4.05 \times 10^{-5}$ ,  $4.26 \times 10^{-5}$  and  $3.2 \times 10^{-5} \text{ mg g}^{-1}$  for 0.5, 1.0, 1.5, 2.0 and 2.5  $\text{mg L}^{-1}$  of As(V), respectively.

### 3.5. IR spectrum studies

IR analysis permits spectrophotometric observation of the adsorbent surface in the range of  $400\text{--}4000 \text{ cm}^{-1}$  and serves as a direct means for the identification of organic functional groups on the surface. An examination of the adsorbent before and after sorption reaction possibly provides information regarding the surface groups that might have participated in the adsorption reaction and also indicates the surface sites on which adsorption has taken place [44]. IR spectrum of PVPCC showed (Fig. 8(I)) peak at  $3426.89 \text{ cm}^{-1}$  that can be assigned to the OH stretching vibration mode of hydroxyl functional groups including hydrogen bond and peaks in the range of  $2935.13 \text{ cm}^{-1}$  indicate the presence of aliphatic OH stretching. The presence of peak at  $1457.92 \text{ cm}^{-1}$  can attribute to the presence of C–H deformation of cyclic  $\text{CH}_2$  groups and peak  $1274.72 \text{ cm}^{-1}$  indicate the presence of C–N stretching. The peak at  $671.106^1$  and  $769.458 \text{ cm}^{-1}$  shows the presence of C–H bend. The C=O bending and C–N stretching mode appears as strong intensity broadband at peak  $1598.7$  and  $1357.64 \text{ cm}^{-1}$ , respectively. These peaks are in coincidence with earlier IR spectrum of PVP [25] depict the presence of PVP coated onto the surface of the cassava carbon.

When As(V) was allowed to adsorb onto the PVP coated cassava carbon broad OH stretching was obtained indicating the presence of intramolecular hydrogen bonding evident by overlapped H-bonded OH peaks between  $3831.86$  and  $3401.82 \text{ cm}^{-1}$ . The intramolecular hydrogen bonding weakens the O–H bond, thereby shifting the band to lower frequency. Further, the presence of As(V) adsorbed to the PVP doped carbon was confirmed by the presence of  $\text{AsO}_2(\text{OH})_2^-$  group at  $873.596 \text{ cm}^{-1}$  (Fig. 8(II)) and were compared to earlier arsenic IR spectrum (Table 4). This peak may be assigned as the symmetric stretching of two equivalent As–O bonds. The enhanced adsorption of As(V) to the PVP coated carbon may also be due to the force constants of As–O bond. As the degree of protonation increases along with  $\text{AsO}_4^{-3}$ ,  $\text{AsO}_3(\text{OH})^{-2}$ ,  $\text{AsO}_2(\text{OH})_2^-$  and  $\text{AsO}(\text{OH})_3$ , the force constant for As–O bond increases indicating that As–O bond is stronger at lower pH leading to stronger

chemical bond. Our results are in agreement with earlier findings [45,46].

### 3.6. X-ray diffraction studies

X-ray diffraction technique is a powerful tool to analyze the nature of the materials. If the material under investigation is crystalline, well-defined peaks are observed while noncrystalline or amorphous system show hallow instead of well-defined peak. Adsorption reaction may lead to change in structure of adsorbent and hence an understanding of the adsorbent and resulting changes thereof would provide valuable information regarding the adsorption reaction [44]. The XRD pattern of PVPCC and As(V) laden PVPCC are presented in Fig. 9. These diffractograms indicate the amorphous nature of the adsorbents indicating that the PVP has diffused into the carbon following which arsenic adsorption has taken place. The amorphous nature of adsorbent before and after As(V) adsorption suggests the possibility of chemisorption reaction.

### 3.7. Desorption studies

The reversibility of As(V) adsorption onto PVPCC was studied at different pH values. The investigation was carried out using spent adsorbent used previously. The desorption of arsenate at different pH is presented in Fig. 4 which shows maximum desorption at pH 11 with 32% As(V) removal. The results suggest that NaOH could be apparently effective desorption agent.

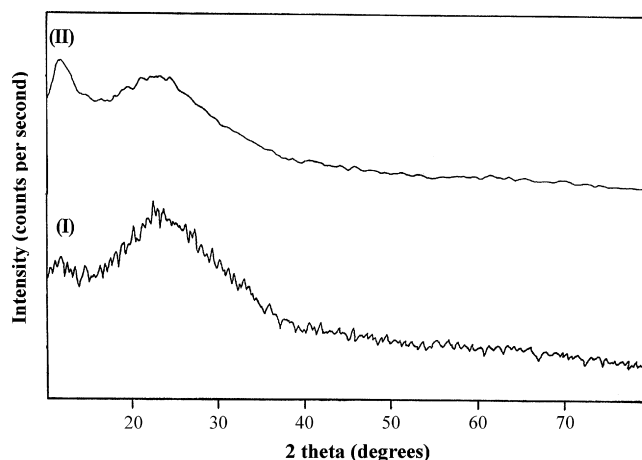


Fig. 9. X-ray diffraction patterns of carbon: (I) X-ray diffraction pattern of PVPCC; (II) X-ray diffraction pattern of As(V) laden PVPCC.

#### 4. Conclusion

The present study showed that PVPCC can be used as an adsorbent for As(V) removal from aqueous solutions whereas As(III) requires prior oxidation to As(V). In batch studies, the adsorption was dependent on initial As(V) concentration and adsorbent dosage. Adsorption of As(V) failed to obey pseudo first order kinetics whereas followed pseudo second order kinetics and was pH dependent. In column mode studies the flow rate, bed height and initial As(V) concentration influenced As(V) adsorption. The  $N_0$  value for As(V) adsorption by PVPCC calculated from BDST model was  $2.59 \times 10^{-5}$ ,  $4.21 \times 10^{-5}$ ,  $4.05 \times 10^{-5}$ ,  $4.26 \times 10^{-5}$  and  $3.2 \times 10^{-5}$  mg g<sup>-1</sup> for 0.5, 1.0, 1.5, 2.0 and 2.5 mg L<sup>-1</sup> of As(V), respectively. The adsorption was higher in batch mode when compared to the column mode studies. The IR studies confirmed the presence of PVP K25 and As(V) on the adsorbent. The XRD studies revealed that the nature of adsorbent was amorphous before and after the As(V) adsorption process. The 32% of As(V) desorption from spent adsorbent was possible at pH 11 using NaOH as desorbing agent. Thus, the PVPCC could be used as an efficient adsorbent for arsenic removal from aqueous solutions.

#### References

- [1] A.I. Zouboulis, I.A. Katsoyiannis, Arsenic removal using iron oxide loaded alginate beads, *Ind. Eng. Chem. Res.* 41 (2002) 6149.
- [2] X. Meng, G.P. Korfiatis, S. Bang, K.W. Bang, Combined effects of anion arsenic removal by iron hydroxides, *Toxicol. Lett.* 133 (1) (2002) 103.
- [3] L. Dambies, Existing and prospective sorption technologies for removal of arsenic in water, *Sep. Sci. Technol.* 39 (3) (2004) 599–623.
- [4] C.P. Huang, P.L.K. Fu, Treatment of arsenic (V)-containing water by the activated carbon process, *J. Water Pollut. Control Fed.* 56 (1984) 233–241.
- [5] P. Mondal, C.B. Majumder, B. Mohanty, Removal of trivalent Arsenic As(III) from contaminated water by calcium chloride (CaCl<sub>2</sub>)-impregnated rice husk carbon, *Ind. Eng. Chem. Res.* 46 (2007) 2550–2557.
- [6] R. Selvakumar, S. Kavitha, K. Swaminathan, Adsorption of As(V) from aqueous solution by chemically doped coir pith carbon, *Ind. J. Chem. Technol.* 14 (2007) 276–282.
- [7] A. Maiti, S. DasGupta, J.K. Basu, S. De, Adsorption of arsenite using natural laterite as adsorbent, *Sep. Purif. Technol.* 55 (2007) 350–359.
- [8] A.B.M. Giasuddin, S.R. Kanel, H. Choi, Adsorption of humic acid onto nanoscale zerovalent iron and its effect on arsenic removal, *Environ. Sci. Technol.* 41 (2007) 2022–2027.
- [9] R.C. Vaishya, S.K. Gupta, Modelling arsenic (III) adsorption from water by sulfate-modified iron oxide coated sand (SMIOCS), *J. Chem. Technol. Biotechnol.* 78 (2002) 73–80.
- [10] K.N. Ghimire, H.I. Yamaguchi, K. Makino, T. Miyajima, Adsorptive separation of arsenate and arsenite from aqueous medium by using orange waste, *Water Res.* 37 (2003) 4945–4953.
- [11] A.M. Raichur, V. Panvekar, Removal of As(V) by adsorption onto mixed rare earth oxides, *Sep. Sci. Technol.* 37 (5) (2002) 1095–1108.
- [12] G.F. Hülya, C.T. Jens, D. Mcconchie, Adsorption of arsenic from water using activated neutralized red mud, *Environ. Sci. Technol.* 38 (2004) 2428–2434.
- [13] M. Sathishkumar, G.S. Murugesan, P.M. Ayyasamy, K. Swaminathan, P. Lakshmanaperumalsamy, Bioremediation of arsenic contaminated groundwater by modified mycelial pellets of *Aspergillus fumigatus*, *Bull. Environ. Contam. Toxicol.* 72 (2004) 617–624.
- [14] G.S. Murugesan, M. Sathishkumar, K. Swaminathan, Arsenic removal from groundwater by pretreated waste tea fungal biomass, *Bioresour. Technol.* 97 (3) (2006) 483–487.
- [15] C.T. Kamala, K.H. Chu, N.S. Chary, P.K. Panday, S.L. Ramesh, A.R.K. Sashtry, K. Chandra Sekar, Removal of arsenic (III) from aqueous solution using fresh and immobilized plant biomass, *Water Res.* 39 (2005) 2815.
- [16] Z. Gu, B. Deng, J. Yang, Synthesis and evaluation of iron containing ordered mesoporous carbon (FeOMC) for arsenic adsorption, *Microporous Mesoporous Mater.* 102 (1) (2007) 265–273.
- [17] D. Clifford, C.-C. Lin, Arsenic(III) and arsenic(V) removal from drinking water in San Ysidro, New Mexico, EPA/600/S2-91/011, US EPA, Cincinnati, 1991.
- [18] V. Lenoble, C. Laclautre, B. Serpaud, V. Deluchat, J.C. Bollinger, As(V) retention and As(III) simultaneous oxidation and removal on a MnO<sub>2</sub>-loaded polystyrene resin, *Sci. Total Environ.* 326 (2004) 197–207.
- [19] M.J. DeMarco, A.K. Sengupta, J.E. Greenleaf, Arsenic removal using polymeric/inorganic hybrid sorbent, *Water Res.* 29 (1995) 297–305.
- [20] P. Sylvester, P. Wsterhoff, T. Moller, M. Badruzzaman, O. Boyd, A hybrid sorbent utilizing nanoparticle of hydrous iron oxide for arsenic removal from drinking water, *Environ. Eng. Sci.* 24 (1) (2007) 104–112.
- [21] T.M. Suzuki, D.A.P. Tanaka, M.A.L. Tanco, M. Kanerato, T. Yokoyama, Adsorption and removal of oxo-anions of arsenic and selenium on zirconium (IV) loaded polymer resin functionalised with diethylenetriamine-*N,N,N',N'*-polyacetic acid, *J. Environ. Monit.* 2 (2000) 550–555.
- [22] S. Deng, Y.P. Ting, Removal of As(V) and As(III) from water with PEI modified fungal biomass, *Water Sci. Technol.* 55 (1–2) (2007) 177–185.
- [23] O.M. Vatutsina, V.S. Soldatov, V.I. Sokolova, J. Johann, M. Bissen, A. Weissenbacher, A new hybrid (polymer/inorganic) fibrous sorbent for arsenic removal from drinking water, *React. Funct. Polym.* 67 (2007) 184–201.
- [24] B.L. Rivas, M.D.C. Aguirre, E. Pereira, J.C. Moutet, E.S. Aman, Capacity of cation water soluble polymer in conjugation with ultrafiltration membrane to remove arsenate ions, *Polym. Eng. Sci.* 47 (8) (2007) 1256–1261.
- [25] C.M. Laot, Spectroscopic characterization of molecular interdiffusion at a poly(vinyl pyrrolidone)/vinyl ester interface, M.Sc. Thesis, Department of Chemical Engineering, Virginia Polytechnic Institute and State University, August 1997.
- [26] M.J. Thompson, G.G. Stewart, I.P. McKeown, Lucite TR structure and function, Research Newsletter, International Centre for Brewing and Distilling, Heriot Watt University, Edinburgh, Autumn, <http://www.bio.hw.ac.uk/icbd/icbd.htm>, 2003.
- [27] Y.T.F. Tan, K.O.K. Khiang Peh, O. Al-Hanbali, Investigation of interpolymer complexation between Carbopol and various grades of polyvinylpyrrolidone and effects on adhesion strength and swelling properties, *J. Pharm. Pharmaceut. Sci.* 4 (1) (2001) 7–14.
- [28] D. Gang, S.K. Banerji, T.E. Cleverger, Chromium (VI) removal by modified PVP coated silica gel, in: Proceedings of the 1999 Conference on Hazardous Waste Research, St. Louis, Missouri, 1999, p. p. 64.
- [29] M. Chanda, G.L. Rempel, Poly(4-vinyl pyridine) gel coated on silica. High capacity and fast kinetics in uranyl sulphate recovery, *Ind. Eng. Chem. Res.* 32 (1993) 726–732.
- [30] G.N. Manju, C. Raji, T.S. Aniruthan, Evaluation of coconut husk carbon for the removal of arsenic from water, *Water Res.* 32 (10) (1998) 3062–3070.
- [31] G. Selva kumari, Adsorption of metal ions, Fe(II), Ni(II), Cr(VI) and Hg(II) from aqueous solution and waste waters by maize cob carbon, Ph.D. Dissertation, Department of Chemistry, PSG College of Arts and Science, Bharathiar University, Coimbatore, India, 2002.
- [32] V. Lenoble, V. Deluchat, B. Serpaud, J.C. Bollinger, Arsenite oxidation and arsenate determination by molybdenum blue method, *Talanta* 61 (2003) 267–276.
- [33] R.A. Hutchins, New method simplifies design of activated carbon, *Syst. Chem. Eng.* 80 (1973) 133–138.
- [34] D. Kavitha, C. Namasivayam, Experimental and kinetic studies on methylene blue adsorption by coir pith carbon, *Bioresour. Technol.* 98 (1) (2007) 14–21.
- [35] M. Mohapatra, S.K. Sahoo, S. Anand, R.P. Das, Removal of As(V) by Cu(II), Ni(II) or Co(II) doped goethite samples, *J. Colloid Interface Sci.* 298 (1) (2006) 6–12.
- [36] K.N. Ghimire, K. Inoue, K. Makino, M. Yajima, Adsorptive removal of arsenic using orange juice residue, *Sep. Sci. Technol.* 37 (12) (2002) 2785–2799.

- [37] L. Yang, S. Wu, J.P. Chen, Modification of activated carbon by polyaniline for enhanced adsorption of aqueous arsenate, *Ind. Eng. Chem. Res.* 46 (7) (2007) 213–240.
- [38] S. Lagergren, *Kunglia Svenska Vetenskapsakademiens, Handlingar, Band, 24* (1898) 1.
- [39] Y.S. Ho, G. McKay, Pseudo second order model for sorption processes, *Process Biochem.* 34 (1999) 451–465.
- [40] K. Nadhem, D.C. Hamidi, M. Xiao, G.Q. Mohammed, F. Max, Adsorption kinetics for the removal of chromium(VI) from aqueous solution by adsorbents derived from used tires and sawdust, *J. Chem. Eng.* 84 (2001) 95–105.
- [41] C. Namasivayam, D. Kavitha, Removal of congo red from water by adsorption onto activated carbon prepared from coir pith and agricultural solid waste, *Dyes Pigments* 54 (2002) 47–58.
- [42] K.K. Deepa, M. Sathishkumar, A.R. Binupriya, G.S. Murugesan, K. Swaminathan, S.E. Yun, Sorption of Cr(VI) from dilute solution and wastewater by live and pretreated biomass of *Aspergillus flavus*, *Chemosphere* 62 (2006) 833–840.
- [43] M. Benavente, M. Arevalo, J. Martinez, Speciation and removal of arsenic in column packed with chitosan, *Water Prac. Technol.* (2006), doi:10.2166/wpt.2006.089.
- [44] C. Namasivayam, D. Kavitha, IR, XRD and SEM studies on the mechanism of adsorption of dyes and phenols by coir pith carbon from aqueous phase, *Microchem. J.* 82 (1) (2006) 43–48.
- [45] P. Persson, N. Nilsson, S. Sjoberg, Structure and bonding of orthophosphoric acid at the iron oxide-aqueous interface, *J. Colloid Interface Sci.* 177 (1996) 263–275.
- [46] S. Goldberg, C.T. Johnston, Mechanism of arsenic adsorption on amorphous oxides evaluated using macroscopic measurements, vibrational spectroscopy and surface complexation modeling, *J. Colloid Interface Sci.* 234 (2001) 204–216.
- [47] E.A. Deliyanni, D.N. Bakoyannakis, A.I. Zouboulis, K.A. Matis, Sorption of As(V) ions by akagaeite type nanocrystals, *Chemosphere* 50 (2003) 155–163.
- [48] D.G. Lumsdon, A.R. Fraser, J.D. Russell, N.T. Livesey, New infrared band assignments for the arsenate ion adsorbed on synthetic goethite ( $\alpha$ -FeOOH), *J. Soil Sci.* 35 (1984) 381–386.
- [49] T.H. Hsia, S.L. Lo, C.F. Lin, D.Y. Lee, Chemical and spectroscopic evidence for specific adsorption of chromate on hydrous iron oxides, *J. Colloids Interfaces* A85 (1994) 1–7.